Syntheses, characterizations, X-ray crystal structures, and antibacterial activities of Co(II), Ni(II), and Zn(II) complexes of the Schiff base derived from 5-nitro-2-hydroxybenzaldehyde and benzylamine

Mehdi Amirnasr, Roghayeh Sadeghi Erami, Kurt Mereiter, Kurt Schenk Joß, Soraia Meghdadi & Soheila Abbasi

Taylor & Francis
Taylor & Francis Group

Syntheses, characterizations, X-ray crystal structures, and antibacterial activities of Co(II), Ni(II), and Zn(II) complexes of the Schiff base derived from 5-nitro-2-hydroxybenzaldehyde and benzylamine

MEHDI AMIRNASR*†, ROGHAYEH SADEGHI ERAMI†, KURT MEREITER‡, KURT SCHENK JOß§, SORAIA MEGHDADI† and SOHEILA ABBASI¶

†Department of Chemistry, Isfahan University of Technology, Isfahan, Iran
‡Faculty of Chemistry, Vienna University of Technology, Vienna, Austria
§CCC-IPSB, École Polytechnique Fédérale de Lausanne, Lausanne, Switzerland
¶Department of Biological Sciences, University of Isfahan, Isfahan, Iran

Three new complexes, $[Co^{II}L_2(bzln)_2]$ (**1**), $[Ni^{II}L_2(DMF)_2]$ (**2**), and $[Zn^{II}L_2]$ (**3**), with the bidentate (NO) Schiff base HL = 2-((E)-(benzylimino)methyl)-4-nitrophenol have been synthesized and characterized. $[Co^{II}L_2(bzln)_2]$ (**1**) was initially formed from the reaction of H_2L^1 (*N,N′*-bis(5-nitrobenzaldehyde)-2-aminoben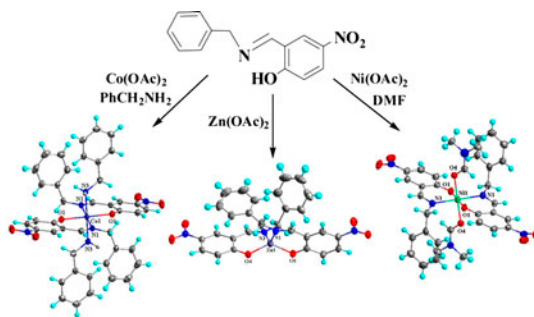zylamine = H_2L^1), with $Co^{II}(CH_3COO)_2 \cdot 4H_2O$ in the presence of benzylamine. The X-ray crystal structure of **1** revealed that HL was formed from the hydrolysis of H_2L^1 and the recondensation of benzylamine with 2-hydroxy-5-nitrobenzaldehyde produced in H_2L^1 hydrolysis. The Schiff base HL was then prepared by direct reaction of 2-hydroxy-5-nitrobenzaldehyde and benzylamine. Complexes **1–3** were also directly synthesized and their crystal and molecular structures determined by X-ray crystallography. The ligand and its metal complexes were also screened for *in vitro* antibacterial activity.

Keywords: Co(II), Ni(II), and Zn(II) complexes; Unsymmetrical Schiff base; Crystal structure; Antibacterial activity

---

*Corresponding author. Email: amirnasr@cc.iut.ac.ir

1. Introduction

Schiff base ligands, defined by Jacobsen as "privileged ligands" [1], are fascinating due to their varying coordination sites, different shapes, functionalities, flexibility, and symmetry. The structural diversity of transition metal complexes of Schiff base ligands and their structure–function relationships have been a focus of attention in recent years [2–8]. A great deal of effort has been directed toward the design and synthesis of functional materials with a variety of applications such as production of highly efficient catalysts [9–13], redox-active sensors [14], ionic ferroelectrics [15], and development of supramolecular architectures with interesting properties [2]. Moreover, they possess a wide variety of biological activity against bacteria, fungi, and certain types of tumors [10–12]. Recently, there has been interest in the synthesis of unsymmetrical Schiff base ligands and their Co(II), Ni(II), and Zn(II) complexes, and investigation of their biological activities [16–21].

In continuation to our recent studies on unsymmetrical Schiff base ligands and their metal complexes [22–24], herein, we report the preparation of the tetradentate unsymmetrical Schiff base H_2nitrosalabza, H_2L^1 [25], and its reaction with cobalt(II) acetate in the presence of benzylamine leading to the octahedral complex $[Co^{II}L_2(bzln)_2]$ (**1**), in which L^- is a bidentate monoanionic ligand produced in the hydrolysis–recondensation process (scheme 1). The direct synthesis and spectroscopic characterization of $[Co^{II}L_2(bzln)_2]$ (**1**) and two other complexes of HL, $[NiL_2(DMF)_2]$ (**2**), and $[ZnL_2]$ (**3**), are also reported (scheme 2). The X-ray crystal structures of **1**, **2**, and **3** and preliminary antibacterial activity of HL ligand and its complexes are also discussed.

2. Experimental

2.1. *Materials and general methods*

All solvents and chemicals were of commercial reagent grade and used as received from Aldrich and Merck. Elemental analyses were performed by using a Perkin–Elmer 2400II CHNS–O elemental analyzer. Infrared spectra (KBr pellets) were recorded on a FT-IR JASCO 680 instrument. ^1H NMR spectra were obtained on a Bruker AVANCE III 400 spectrometer. Proton chemical shifts are reported in ppm relative to an internal standard of Me_4Si. Electronic spectra were obtained on a JASCO V-570 spectrophotometer. The molar conductivity of freshly prepared 1.4×10^{-4} M DMSO solution of the Co(II) complex was measured using a Digital-Konduktometer CG 855 instrument.

2.2. *Synthesis*

2.2.1. Synthesis of ligands. H_2L^1 and HL were prepared as reported in the literature [25, 26]. These ligands were characterized by elemental analysis and spectroscopic methods. The melting points of the ligands are 248–250 °C for H_2L^1 and 148–150 °C for HL. FT-IR: (KBr pellet, cm^{-1}): 1650 s (υ C=N). UV–Vis: λ_{max} (nm) (ε, M^{-1} cm^{-1}) (DMF): 426 (14,633), 364 (11,193). ^1H NMR (DMSO-d_6, 400 MHz), δ (ppm): 14.52 (1H, OH), 8.91 (1H, CH=N), 6.70–8.48 (8H, ArH), 3.33 (2H, CH_2 benzylic).
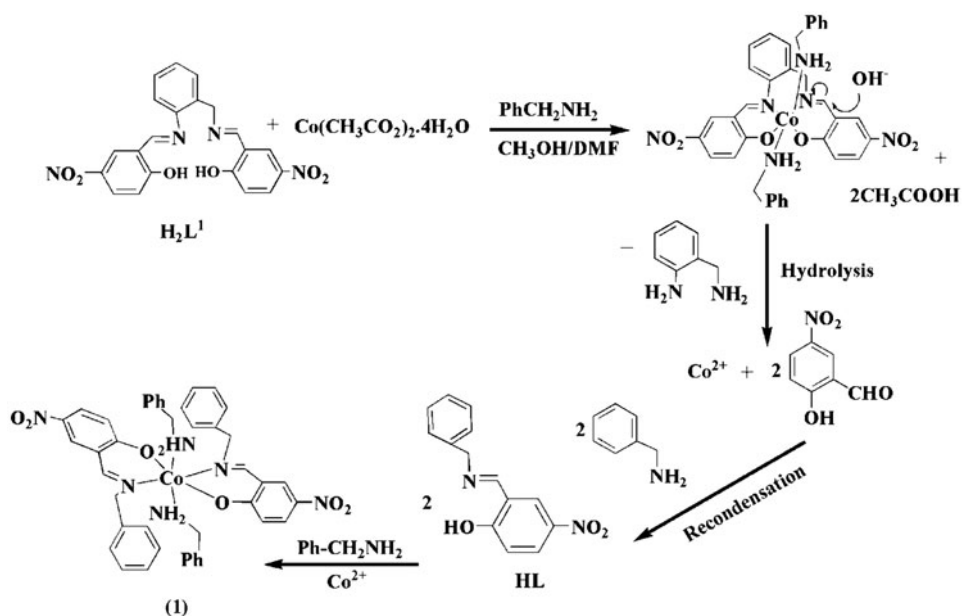
Scheme 1. Formation of HL and its Co(II) complex in the hydrolysis–recondensation reaction of H_2L^1.
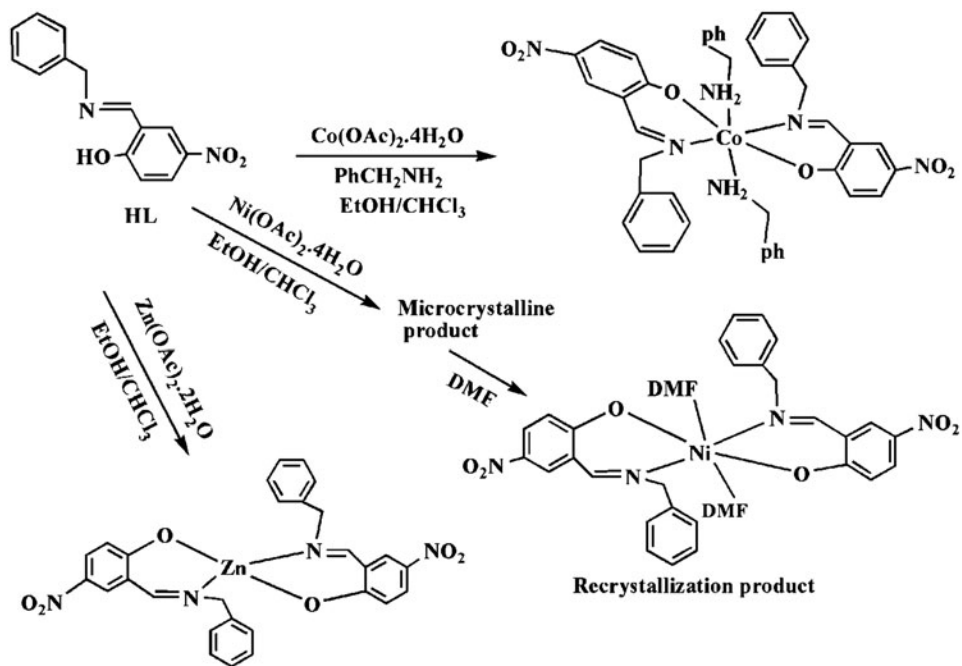
Scheme 2. Direct synthesis of the Co(II), Ni(II), and Zn(II) complexes from HL.

2.2.2. Synthesis of [Co^{II}L$_2$(bzln)$_2$] (1). To a stirring solution of Co(CH$_3$COO)$_2$·4H$_2$O (24.9 mg, 0.1 mmol) in 10 mL ethanol was added a solution of L (51.2 mg, 0.2 mmol) in 15 mL CHCl$_3$ at room temperature. To this solution, 3.0 mmol of benzylamine was added dropwise within 3 h. The final reaction mixture was filtered off and the filtrate was left undisturbed at room temperature for three days. The resulting yellowish brown crystals of **1** suitable for X-ray crystallography were filtered off and washed with cold ethanol and dried under vacuum. Yield 73%. Anal. Calcd for C$_{42}$H$_{40}$N$_6$O$_6$Co (%): C, 64.36; H, 5.14; N, 10.72. Found: C, 64.14; H, 5.06; N, 10.42. FT-IR (KBr pellet, cm^{-1}): 3283 and 3336 m (υ NH$_2$). 1632 s (υ C=N), UV–Vis: λ_{max} (nm) (ε, M^{-1}cm^{-1}) (DMF): 577 (232), 390 (23,686).

2.2.3. Synthesis of [NiL$_2$(DMF)$_2$] (2). A solution of the ligand (51.2 mg, 0.2 mmol) in 15 mL CHCl$_3$ was added to a stirring solution of Ni(CH$_3$COO)$_2$·4H$_2$O (24.8 mg, 0.1 mmol) in 15 mL ethanol. The solution turned green immediately and the product precipitated as microcrystalline solid. The precipitate was filtered off and washed with cold ethanol. Dark green crystals of **2** suitable for X-ray analysis were obtained by recrystallization of the product in DMF after seven days. The crystals were filtered off and washed with cold ethanol. Yield 79%. Anal. Calcd for C$_{34}$H$_{36}$N$_6$O$_8$Ni (%): C, 57.08; H, 5.07; N, 11.75. Found: C, 57.21; H, 5.14; N, 11.42. FT-IR (KBr pellet, cm^{-1}): 1615 s (υ C=O$_{DMF}$), 1604 s (υ C=N), UV–Vis: λ_{max} (nm) (ε, M^{-1}cm^{-1}) (DMF): 594(136), 420 (1920), 309 (22,600).

2.2.4. Synthesis of [ZnL$_2$] (3). To a stirring solution of Zn(CH$_3$COO)$_2$·2H$_2$O (10.95 mg, 0.05 mmol) in 15 mL ethanol was added a solution of the ligand (25.7 mg, 0.1 mmol) in 15 mL CHCl$_3$. The solution turned yellow after 4 h. Yellow crystals of **3** were obtained during a week by slow evaporation of the solvent in open air. The crystals were filtered off and washed with cold ethanol. Yield 75%. Anal. Calcd for C$_{28}$H$_{22}$N$_4$O$_6$Zn (%): C, 58.40; H, 3.85; N, 9.73. Found: C, 58.83; H, 3.90; N, 9.73. FT-IR (KBr pellet, cm^{-1}): 1631s (υ C=N). UV–Vis: λ_{max} (nm) (ε, M^{-1}cm^{-1}) (DMF): 364 (3252). ^{1}H NMR (DMSO-d$_6$, 400 MHz), δ (ppm): 8.39 (2H, CH=N), 6.49–8.20 (16H, ArH), 4.59 (4H, CH$_2$ $_{benzylic}$).

2.3. Crystal structure determination

2.3.1. X-ray crystallography for 1 and 3. Yellowish brown crystals of **1** and yellow crystals of **3** grown as described above were used for X-ray crystallography. Diffraction data of **1** and **3** were collected at T = 100 and 297 K, respectively, on a Bruker Smart APEX CCD diffractometer with graphite-monochromated MoKα radiation (λ = 0.71073 Å). After cell refinement and data reduction with SAINT, a multi-scan absorption correction was applied to the data with SADABS [27]. The structures were solved with direct methods (SHELXS [28]) and refined on F^2 using SHELXL-97 [28]. Hydrogen was placed at geometrically calculated positions and refined using a riding model with fixed C–H and N–H distances. Details of crystallographic data and refinement of the complexes are summarized in table 1, while selected bond lengths and angles are presented in table 2. A list of hydrogen bonds is given in table 3.

2.3.2. X-ray crystallography for 2. Green crystals of **2** suitable for X-ray crystallography were grown by slow evaporation of a DMF solution of the complex at room temperature.

Table 1.   Crystal data and structure refinement parameters for **1**, **2**, and **3**.

Chemical formula	$C_{42}H_{40}N_4O_6Co$ (**1**)	$C_{34}H_{36}N_6O_8Ni$ (**2**)	$C_{28}H_{22}N_4O_6Zn$ (**3**)
Formula weight	783.73	715.40	575.87
Temperature (K)	100(2)	293(2)	297(2)
Crystal system, space group	Triclinic, $P\bar{1}$	Triclinic, $P\bar{1}$	Triclinic, $P\bar{1}$
a (Å)	8.1957(2)	7.3179(15)	10.8435(3)
b (Å)	10.5961(2)	10.584(2)	11.6089(3)
c (Å)	11.4164(2)	12.114(2)	11.9706(3)
α (°)	70.634(1)	110.74(3)	90.305(2)
β (°)	84.588(1)	98.74(3)	114.832(2)
γ (°)	83.617(1)	98.13(3)	105.902(2)
V (Å^3)	927.79(3)	847.7(3)	1302.65(6)
Z, Calculated density (g/cm^3)	1, 1.403	1, 1.401	2, 1.468
Crystal size (mm)	0.36 × 0.34 × 0.16	0.26 × 0.11 × 0.10	0.55 × 0.14 × 0.08
μ (mm^{-1})	0.52	0.63	0.99
$F(0\,0\,0)$	409	374	592
θ range (°)	2.0–30.0	1.8–25.5	1.8–28.3
Index ranges	$-11 \leq h \leq 7, -14 \leq k \leq 14, -16 \leq l \leq 16$	$-8 \leq h \leq 8, -12 \leq k \leq 12, -14 \leq l \leq 14$	$-14 \leq h \leq 14, -12 \leq k \leq 15, -15 \leq l \leq 15$
Reflns. collected/unique/R_{int}	8950/5267/0.017	5715/2944/0.117	17,573/6416/0.025
Absorption correction	Multi-scan	Numerical	Multi-scan
Min. and max. transmission	0.79, 0.92	0.885, 0.957	0.84, 1.00
Data/restraints/parameters	5267/0/250	2944/0/223	6416/0/352
Goodness-of-fit on F^2	1.035	0.995	1.02
Final R indices $[I > 2\sigma(I)]$	$R_1 = 0.043$, $wR_2 = 0.103$	$R_1 = 0.101$, $wR_2 = 0.261$	$R_1 = 0.046$, $wR_2 = 0.122$
R indices (all data)	$R_1 = 0.055$, $wR_2 = 0.111$	$R_1 = 0.127$, $wR_2 = 0.288$	$R_1 = 0.062$, $wR_2 = 0.132$
Max./min. $\Delta\rho$ (e Å^{-3})	0.79 and -0.23	1.67 and -1.23	0.84 and -0.21

Table 2. Selected bond lengths (Å) and angles (°) for **1**, **2**, and **3**.

[Co^{II}L$_2$(bzln)$_2$] (**1**)		[NiL$_2$ (DMF)$_2$] (**2**)		[ZnL$_2$] (**3**)	
Bond lengths					
Co1–O1	2.0457(11)	Ni1–O1	2.025(5)	Zn1–O4	1.9278(16)
Co1–O1^{ia}	2.0457(11)	Ni1–O1^{ia}	2.025(5)	Zn1–O1	1.9286(16)
Co1–N1	2.1428(13)	Ni1–N1	2.105(5)	Zn1–N1	1.996(2)
Co1–N1^i	2.1428(13)	Ni1–N1^i	2.105(5)	Zn1–N3	1.996(2)
Co1–N3	2.1878(13)	Ni1–O4	2.101(4)		
Co1–N3^i	2.1878(13)	Ni1–O4^i	2.101(4)		
O1–C2	1.2866(18)		1.268(7)		1.293(3)/1.297(3)^b
O2–N2	1.2402(19)		1.230(12)		1.239(3)/1.232(3)
O3–N2	1.2405(19)		1.222(12)		1.226(3)/1.231(3)
C1–C7	1.452(2)		1.444(11)		1.445(3)/1.458(3)
N1–C7	1.282(2)		1.287(9)		1.280(3)/1.277(3)
N1–C8	1.479(2)		1.477(10)		1.473(3)/1.479(3)
Bond angles					
O1–Co1–O1^i	180.00	O1–Ni1–O1^i	180.0	O1–Zn1–O4	128.46(8)
O1–Co1–N1	88.27(5)	O1–Ni1–N1	89.0(2)	O1–Zn1–N1	95.76(8)
O1–Co1–N1^i	91.73(5)	O1–Ni1–N1^i	91.0(2)	O1–Zn1–N3	107.37(8)
O1–Co1–N3	92.34(5)	O1–Ni1–O4	90.0(2)	O4–Zn1–N1	105.78(8)
O1–Co1–N3^i	87.66(5)	O1–Ni1–O4^i	90.0(2)	O4–Zn1–N3	96.55(7)
N1–Co1–N1^i	180.00	N1–Ni1–N1^i	180.0	N1–Zn1–N3	126.32(9)
N1–Co1–N3	90.46(5)	N1–Ni1–O4	93.2(2)		
N1–Co1–N3^i	89.54(5)	N1–Ni1–O4^i	86.8(2)	C2–O1–Zn1	124.04(15)
N3–Co1–N3^i	180.00	N3–Ni1–O4^i	180.00	C16–O4–Zn1	122.94(14)

^{a}Symmetry code: (i) = −x, −y, −z.
^{b}Second value reports equivalent bond lengths for the second ligand.

Table 3. Hydrogen bond lengths (Å) and angles (°) for **1**, **2**, and **3**.

D–H···A	d(D–H)	d(H···A)	d(D···A)	D–H···A
[Co^{II}L$_2$(bzln)$_2$] (**1**)				
N3–H3A···O2^{ia}	0.92	2.51	3.425(2)	175
N3–H3A···O3^{ia}	0.92	2.53	3.192(2)	129
N3–H3B···C9^b	0.92	2.74	3.459(2)	135
N3–H3B···C10^b	0.92	2.80	3.477(2)	131
[Ni^{II}L$_2$(DMF)$_2$] (**2**)				
C16–H16C···O2^{ii}	0.96	2.49	3.358(12)	150
[Zn^{II}L$_2$] (**3**)				
C3–H3···O5^{iii}	0.93	2.59	3.439(3)	152
C11–H11···O6^{iv}	0.93	2.49	3.286(4)	143
C17–H17···O2^v	0.93	2.55	3.398(3)	152
C21–H21···O3^{vi}	0.93	2.44	3.354(3)	166

Note: Symmetry codes: (i) x, y, 1 + z; (ii) −x, −y, 1 − z; (iii) −x, −y, −z; (iv) −x, 1 − y, −z; (v) 1 − x, −y, 1 − z; (vi) x − 1, y, z − 1.
^{a}Bifurcated N–H···O, O bond.
^{b}C–H···π bond.

Bragg intensities from **2** were collected at T = 293 K on a Stoe IPSD II image plate system with graphite monochromated MoKα radiation (λ = 0.71073 Å). Cell refinement and data reduction were performed with the X-AREA program (1.62) [29]. Absorption factors were obtained by numerical integration in XRED 32 (1.31) [30]. The structure was solved with the help of DIRDIF [31] and was refined like **1** and **3** on F^2 using SHELXL-97 [28].

Crystal data and details of the refinement are summarized in table 1, while selected bond lengths and angles are presented in tables 2 and 3.

2.4. *Antibacterial activity*

Antibacterial activities of the ligand and its complexes were tested by the well-known diffusion method using Sabouraud dextrose agar and Müller Hinton agar [32]. Stock solutions of HL and **1–3** were prepared in DMSO. The zone of inhibition was recorded on the completion of the incubation as the mean diameter (MZI) for each complex at 650 μg mL^{-1} (~1 mM). The MIZ produced by the compounds were compared with the standard antibiotic Penicillin of 1 mM concentration. Each test was carried out three times to minimize the error. In order to clarify any effect of DMSO in the biological screening, blank studies were carried out, and no activity was observed against any bacterial strains in pure DMSO.

3. Results and discussion

3.1. *Synthesis*

The *trans*-[Co^{II}L$_2$(bzln)$_2$] complex was obtained unexpectedly as the product of an attempted synthesis of [Co^{III}(L^1)(bzln)$_2$]$^+$ from the reaction between cobalt(II) acetate and the tetradentate Schiff base ligand H$_2$L^1 in the presence of benzylamine (scheme 1). Literature reports [33] show that metal complexes of Schiff base ligands may undergo hydrolysis resulting in new products of rearranged Schiff base ligands. Factors such as metal ions, ligand systems, solvents, and anions can have a marked influence on the reaction path. We have recently demonstrated the effect of counteranions of the metal salts on the hydrolysis of a tridentate unsymmetrical Schiff base HBacabza = 3-(2-aminobenzylimino)-1-phenylbutan-1-one in the presence of Cu(ClO$_4$)$_2$·6H$_2$O in methanol and recondensation to its isomer 3-(2-aminomethylphenyleneimino)-1-phenylbutan-1-one [23]. The results of the aforementioned transformation of the tetradentate H$_2$L^1 to the bidentate ligand HL during *trans*-[Co^{II}L$_2$(bzln)$_2$] formation inspired us to synthesize and fully characterize Co(II), Ni(II), and Zn(II) complexes of the bidentate Schiff base ligand HL, derived directly from 5-nitro-2-hydroxybenzaldehyde and benzylamine. These complexes were obtained in good yields of 73% for **1**, 79% for **2,** and 75% for **3**. The complexes were characterized using different spectroscopic methods and X-ray crystallography. In DMSO, the cobalt complex is a non-electrolyte as reflected in its low Λ_M value (11.5 Ω^{-1} cm^2 M^{-1}) [34, 35].

3.2. *Spectral characterization*

The newly prepared metal complexes are all air-stable solids and have good elemental analyses. The octahedral geometry of Co and Ni in **1** and **2**, and also tetrahedral geometry of Zn in **3**, are evident from the X-ray structure analysis (figures 1, 3 and 4). FT-IR data of the complexes are listed in Section 2. Significant information regarding the bonding sites of ligand can be obtained by comparing the IR spectra of the metal complexes with the free ligand. A strong absorption at 1632 cm^{-1} for **1**, 1604 cm^{-1} for **2,** and 1631 cm^{-1} for **3** is assigned to ν(C=N) of the coordinated imine. These bands are at lower frequencies relative to that of the free Schiff base, HL (1650 cm^{-1}), indicating a decrease in C=N bond order
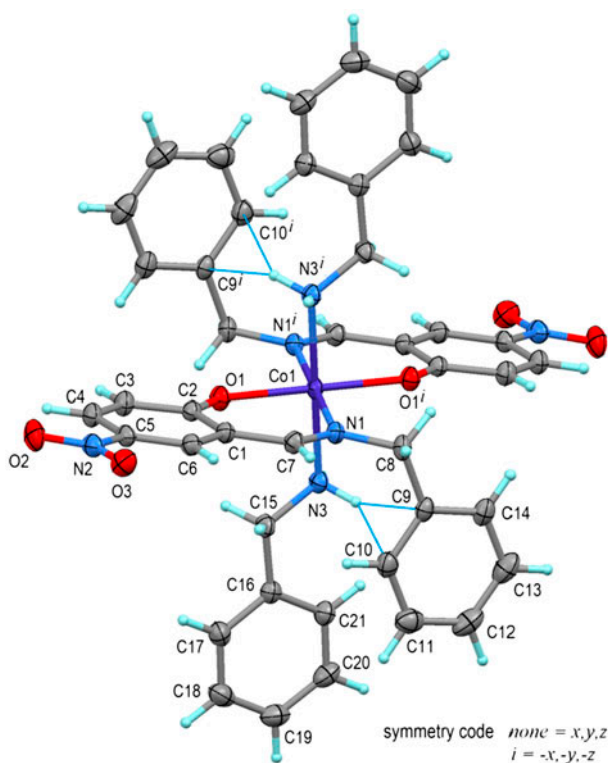
Figure 1. The molecular structure of $[Co^{II}L_2(bzln)_2]$ (**1**) with atom labeling scheme. Displacement ellipsoids are drawn at 50% probability. The complex is centrosymmetric with Co in *x, y, z* = 0, 0, 0. The thin blue lines indicate intramolecular N–H···π bonding (N3···C9 = 3.459(2), N3···C10 = 3.477(2) Å) (see http://dx.doi.org/10.1080/00958972.2014.996144 for color version).

due to coordination of the imine nitrogen to the metal and back bonding from the metal to the π^* orbitals of the azomethine groups. A band at 1615 cm^{-1} in the spectrum of **2** is assigned to ν(C=O) of coordinated DMF. Free DMF exhibits a band at 1680 cm^{-1} due to ν(C=O), which shifts to lower frequencies in spectra of O-bonded DMF metal complexes, indicating amide oxygen coordination [36]. These results conform to the structural data obtained by X-ray crystallography.

The UV–Vis data are presented in the experimental section. The electronic absorption spectrum of HL and complexes were recorded using DMF as the solvent. The electronic spectrum of HL in DMF shows a band at 426 nm (ε = 14,633 M^{-1} cm^{-1}) and a band in the UV region at 364 nm (ε = 11,193 M^{-1} cm^{-1}) corresponding to the intramolecular π–π^* and n–π^* transitions. Characteristic bands for the complexes were also detected as follows. The electronic absorption spectrum of **1** shows an IL-CT band at 390 nm (ε = 23,686 M^{-1} cm^{-1}) and a band in the visible region at 577 nm (ε = 232 M^{-1} cm^{-1}) corresponding to the ligand field transition of the cobalt(II) complex. The electronic spectrum of **2** shows one band at 309 nm (ε = 22,600 M^{-1} cm^{-1}) and two bands at 420 nm (ε = 1920 M^{-1} cm^{-1}) and 594 nm (ε = 136 M^{-1} cm^{-1}), assigned to the charge-transfer and the ligand field [$^3A_{2\,g} \rightarrow {}^3T_{1\,g}(F)$] transitions, respectively. Complex **3** shows one band at 364 nm (ε = 3252 M^{-1} cm^{-1}), which may be attributed to the intramolecular or charge-transfer transitions.
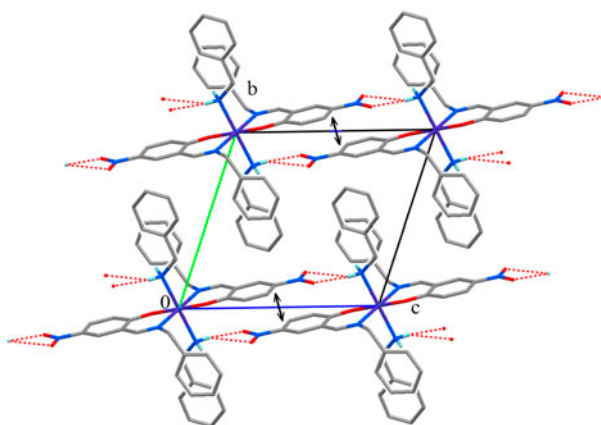
Figure 2. Packing and intermolecular interactions in the crystal structure of **1** viewed along [1 0 0].

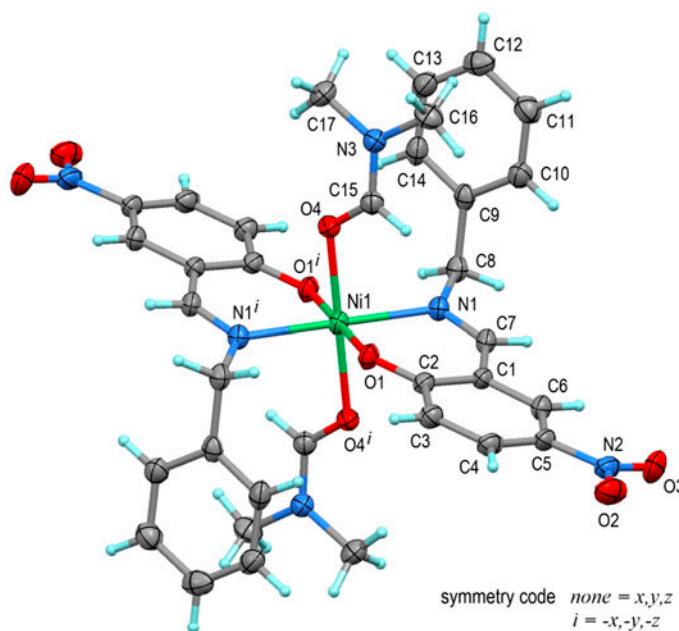symmetry code *none = x,y,z*
i = -x,-y,-z

Figure 3. The molecular structure of **2** with atom labeling scheme. Displacement ellipsoids are drawn at 20% probability. The complex is centrosymmetric with Ni in *x, y, z* = 0, 0, 0. The distance between N3 and the centroid of ring C9–C14 is 3.50 Å.

^{1}H NMR spectral measurements were performed in DMSO-d_6 for L and its Zn(II) complex and the spectroscopic data are given in the experimental section. As expected, the OH of the ligand is at 14.42 ppm as a broad singlet due to intramolecular hydrogen

bonding. The singlet at 8.91 ppm corresponds to the methylidene proton. The signals corresponding to the eight aromatic protons resolve in the range 6.70–8.48 ppm, and the benzylic (CH_2) protons appear at 3.33 ppm. The spectrum of the zinc complex features a singlet at 8.39 ppm for the methylidene protons. The signals at 6.49–8.20 ppm for **3** are attributed to the sixteen aromatic protons of the two monoanionic bidentate (L^-) ligands, coordinated to the zinc center. The benzylic (CH_2) protons appear as a singlet at 4.59 ppm.

3.3. *Crystal structure of [Co^{II}L$_2$(bzln)$_2$] (1)*

The molecular structure and atom numbering scheme of **1** is presented in figure 1. Selected bond distances and angles are given in tables 2 and 3. This complex crystallizes in triclinic space group *P*$\bar{1}$ with Co located on a center of inversion and coordinated in an octahedral fashion. As expected, HL is a bidentate mono-anionic ligand and binds to the cobalt ion via phenolate O1 and imine N1 so that O1, O1^i, N, and N1^i are in equatorial positions. The two axial sites are occupied by the amine nitrogens N3 and N3^i of two benzylamine molecules. The bond lengths Co–N1=Co–N1^i=2.1428(13) Å and Co–O1=Co–O1^i=2.0457(11) Å are comparable to the average bond distances Co–N (2.121(3) Å) and Co–O (2.097(3) Å) observed in a related Co(II) complex [37]. The two axial bond distances Co1–N3=Co–N3^i = 2.1878(13) Å are longer than the equatorial bond distances due to different donor/back donation properties of the axial and equatorial ligands, and a weak Jahn–Teller effect. A comparison of the observed Co–N, O bond lengths in **1** with those of related complexes in the Cambridge Crystallographic Database indicates that cobalt is d^7 high-spin with three unpaired electrons. Similar Co–N bond distances (2.1272(15) and 2.0671(19) Å) in high spin cobalt(II) complex [Co(pbba)$_2$(NCS)$_2$], pbba = N-((pyridine-yl-)benzylidene)benzyl-amine, are reported [38]. Molar conductivity measurements gave additional support to the molecular and non-electrolyte nature of [Co^{II}L$_2$(bzln)$_2$] complex (*vide supra*).

All three *trans* angles about Co are ideal 180°. The six-membered chelate ring formed by phenolate-O and imine-N has a bite angle of O1–Co1–N2 = 88.27(5)°. The bond angles between equatorial and axial ligands deviate only by ±0.46(5)° and ±2.34(5)° from 90°. The 2-oxy-5-nitrobenzylidenimine moiety is nearly flat showing a rms deviation from planarity of 0.034 Å with Co deviating by 0.371(1) Å from this plane. It encloses interplanar angles of 87.8(4)° and 87.7(4)° with the phenyl rings C9–C14 and C16–C21, respectively, the latter two being almost parallel to each other with an interplanar angle of only 4.7(1)°. The shortest intramolecular approach between these two phenyl rings is C11···C21 = 3.559(3) Å (figure 1) but their ring–ring overlap is too small to consider this a significant π–π interaction. However, there is a stabilizing intramolecular N–H···π type hydrogen bond interaction between NH$_2$ and the phenyl ring C9–C14, with N3···C9 = 3.459(2) Å and N3···C10 = 3.477(2) Å (thin blue lines in figure 1 and table 3). In the crystal lattice, the complexes are aligned with their phenyl rings C9–C14 and C16–C21 in layers parallel to (222), and with their 2-oxy-5-nitrobenzylidenimine moieties oriented parallel to (1-3-1), i.e. approximately perpendicular to (2 2 2). These layers repeat in both directions every 3.3 Å and enable intermolecular slipped π–π interactions between centrosymmetric pairs of nitro-phenyl moieties with an interplanar distance of 3.179 Å (shown as double arrows in figure 2), and between the phenyl rings C9–C14 at *x*, *y*, *z* and C16–C21 at 1−*x*, −*y*, −*z* with a corresponding distance of 3.490 Å, effective in view of the direction to which these rings are inclined by ca. 30° (figure 2). Further coherence of the crystal lattice is provided by an intermolecular bifurcated N–H···O, O hydrogen bond between the amino group and the two nitro oxygens O2 and O3 as acceptors (red dashed lines in figure 2 and table 3).

3.4. *Crystal structure of [NiL₂(DMF)₂] (2)*

The molecular structure and atom numbering scheme of **2** is presented in figure 3. The crystallographic data and structure analysis for this complex are summarized in table 1. Selected bond distances and angles are given in table 2. This complex crystallizes in triclinic space group $P\bar{1}$ and its metal ion is in an octahedral environment containing two N1 and two O1 donors of two L⁻ ligand in the equatorial positions and two oxygens (O4) of DMF in the axial positions. Like **1**, **2** is also centrosymmetric and, therefore, *trans* bond distances are identical and *trans* bond angles are 180°. The bond distances Ni1–N1 = 2.110(6) Å, Ni1–O1 = 2.025(5) Å, and Ni1–O4 = 2.101(5) Å are comparable to the average bond distances Ni–N (2.012(5) Å) and Ni–O (1.998(4) Å) observed in a related Ni(II) complex [39].

The chelate bite angle formed by phenolate-O and the imine-N, O1–Ni1–N1 = O1ⁱ–Ni1–N1ⁱ = 89.0(2)°, is similar to **1**. The *cis* bond angles to DMF O4 are 90.0(2)° (O1) and 90 ± 3.2(2)° (N1). The DMF is near parallel to the adjacent phenyl ring C9–C14 (interplanar angle 5.9°) and both are approximately perpendicular to the nitrophenyl moiety (89.7° and 84.1°, respectively). In the crystal lattice, DMF ligands and phenyl rings C9–C14 form continuous stacks along the *a* axis with weak C–H⋯π interactions not included in table 3 because of their excessive length (C⋯C > 3.6 Å). Further coherence of the complexes in the crystal lattice is provided by slipped π–π interactions between pairs of nitrophenyl moieties (perpendicular distance 3.403(3) Å) and a C–H⋯O (nitro) hydrogen bond (table 3). The crystal of **2** shows some similarities to that of **1**.

3.5. *Crystal structure of [ZnL₂] (3)*

The molecular structure and atom numbering scheme of **3** is presented in figure 4. The crystallographic data for this complex are summarized in table 1. Selected bond distances and angles are given in table 2. Like **1** and **2**, **3** crystallizes in the triclinic space group $P\bar{1}$, but unlike **1** and **2,** the Zn complex **3** is not centrosymmetric and there are two complexes instead of one in the unit cell. Zn(II) is coordinated by four N, O-donors: two nitrogens (N1, N3) from imino groups and two oxygens (O1, O4) from phenolates of L⁻, respectively. The coordination environment around Zn(II) is a distorted tetrahedron. All Zn–N and Zn–O bond distances are within the normal range observed in other four-coordinate zinc(II) complexes. The bonds Zn–N1 and Zn–N3 (1.996(2) Å) are equal and compare well with the average Zn–N bond lengths in [Zn(L¹)₂] (2.006 Å) [40]. The bond distances Zn–O1 (1.9286(16) Å) and Zn–O4 (1.9278(16) Å) are very close and are also in agreement with the Zn–O bond distance (1.942(6) Å) in [Zn(L¹)₂] [40].

The two chelate angles O1–Zn1–N1 (95.76(8)°) and O4–Zn1–N3 (96.55(7)°) formed by the phenolate-O and the imine-N are similar and close to those reported for the related [Zn(L¹)₂]. The remaining bond angles in the ZnN₂O₂ tetrahedron are either near the ideal tetrahedral angle 109.47° for O1–Zn–N3 and O4–Zn–N1, or very big for O1–Zn–O4 (128.46(8)°) and N1–Zn1–N3 (126.32(9)°) showing that the tetrahedron is considerably compressed along the vertical axis (figure 4). While the ZnN₂O₂ tetrahedron and the two independent 2-oxy-5-nitrobenzylidenimine moieties (C1–C7, N1–N2, O1–O3, and C15–C21, N3–N4, O4–O6) define a nearly C_2-symmetric arrangement (C_2 axis through the centroid of N1 and N3 and the centroid of O1 and O4, the compression axis of the ZnN₂O₂ tetrahedron), the two benzyl residues C8–C14 and C22–C28 adopt an asymmetric arrangement where ring C9–C14 is near parallel to ring C15–C20 (interplanar angle 12.5(2)°) and ring C23–C28 is steeply inclined to ring C1–C6 (interplanar angle 49.2(2)°).
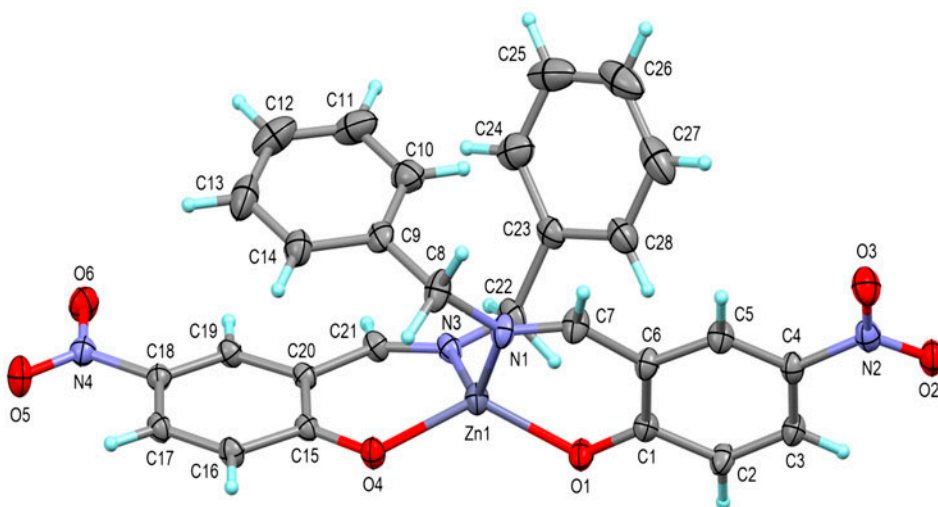
Figure 4. The molecular structure of **3** with atom labeling scheme. Displacement ellipsoids are drawn at 20% probability.

The two 2-oxy-5-nitrobenzylidenimine moieties have rms deviations from planarity of 0.076 and 0.045 Å with Zn by 0.477(2) and 0.472(2) Å displaced from these planes. They subtend an interplanar angle of 76.43(4)°.

Intermolecular interactions in the crystal lattice of **3** comprise slipped π–π stacking between centrosymmetric pairs of 2-oxy-5-nitrobenzylidenimine moieties with C···C,O distances of 3.54–3.61 Å, two interesting sides on contacts between each NO_2 group and a phenolate oxygen with N···O = 3.0–3.11 Å, and two C–H···O interactions to each nitro group. These interactions, shown in figure 5, generate infinite molecular chains that extend parallel to [1 0 1] through the crystal lattice. Contact distances are (Å): C1–C2^{ii} 3.539(4), C7–C3^{ii} 3.538(4), C6–O1^{ii} 3.605(3), N2–O4^{ii} 3.114(3), O2–C17^{ii} 3.398(3) (ii = 1 − x, −y, 1 − z), C15–C16^{i} 3.574(3), C21–C17^{i} 3.536(3), C20–O4^{i} 3.612(3), N4–O1^{i} 3.089(3), O5–C3^{i} 3.439 (3) (i = −x, −y, −z), where O2–C17^{ii} and O5–C3^{i} represent C–H···O bonds. The cross-linking of these chains perpendicular to [1 0 1] is less organized and involves, apart from unremarkable van der Waals contacts, only two further C–H···O bonds from the benzyl groups to nitro oxygens, C11···O6 (−x, 1 − y, −z) = 3.286(4) Å and C11···O6 (x − 1, y, z − 1) = 3.354(3) Å. The π–π stacking between centrosymmetric pairs of nitrophenyl fragments is common to **1**, **2**, and **3**. However, the mutual overlap of the fragments is notably bigger in **3** than in **1** and **2**, with the effect that it includes here the phenolate O and the imine carbon.

3.6. *Antibacterial activity*

The ligand and its metal complexes were tested for antibacterial activity against *Bacillus cereus* and *Staphylococcus aureus* as Gram +ve and *Salmonella typhi*, *Klebsiella pneumoniae*, and *Escherichia coli* as Gram –ve species. The screening results (minimum zone of inhibition, MZI) are summarized in table 4. The data revealed that, though no significant activity is observed against the Gram –ve species, the activity of the ligand is enhanced against the Gram +ve bacteria upon coordination. Both complexes, **1** (MZI = 30 mm) and **2**
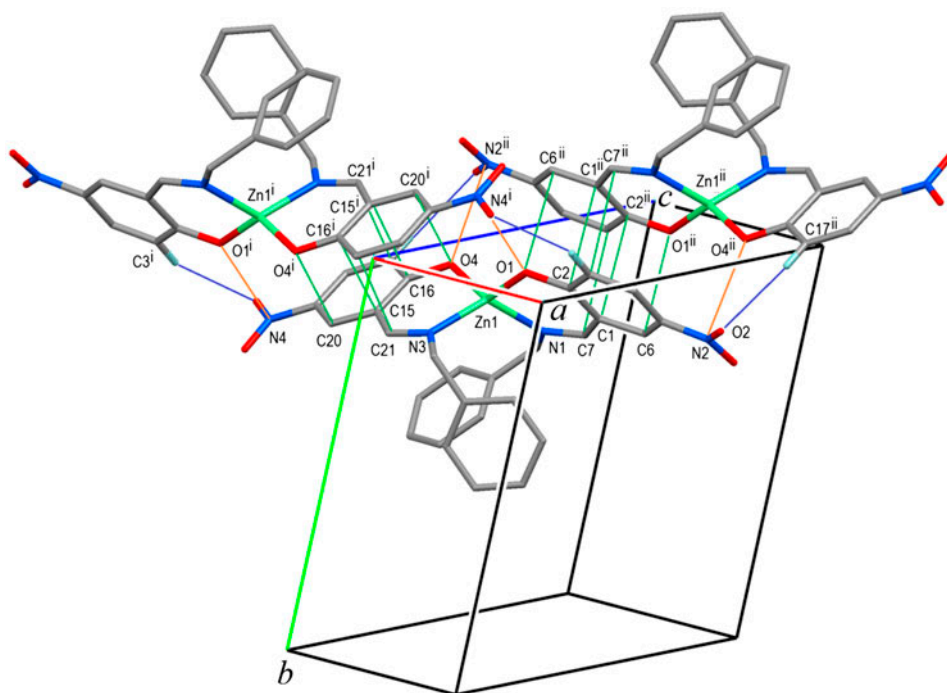
Figure 5. Three molecules of **3** and their interactions, mainly π–π stacking type, to form an infinite chain extending parallel to [101]. Short intermolecular C–C and C–O contacts are indicated by thin green lines, N–O contacts by orange lines, and C–H···O bonds by thin blue lines. Only hydrogens involved in these interactions are shown (see http://dx.doi.org/10.1080/00958972.2014.996144 for color version).

Table 4. MZI (mm) for the antimicrobial activity of HL, **1**, **2**, and **3**.

Compound	*Bacillus cereus*	*Staphylococcus aureus*	*Salmonella typhi*	*Klebsiella pneumoniae*	*Escherichia coli*
HL	17	8	10	8	8
[Co^{II}L$_2$(bzln)$_2$] (**1**)	13	30	None	7	None
[Ni^{II}L$_2$(DMF)$_2$] (**2**)	15	28	None	None	None
[Zn^{II}L$_2$] (**3**)	None	18	13	15	None
Penicillin	20	33	18	20	25
DMSO	None	None	None	None	None

(MZI = 28 mm), exhibit antibacterial activity against *Staphylococcus aureus* comparable to that observed for penicillin, MZI = 33 mm (figures 6 and 7; table 4). Moreover, the antibacterial effect of these two complexes on *Staphylococcus aureus* is higher than that reported for related complexes (MZI = 14.0 mm for Co^{II}L^2 [41], 17 mm for Co^{II}AFL, and 18 mm for Ni^{II}AFL [42]).

In the metal complex, the polarity of the metal ion is presumably reduced due to overlap of the ligand orbital and partial sharing of the positive charge of the metal ion with donor groups. Furthermore, the increased delocalization of π electrons over the whole chelate ring
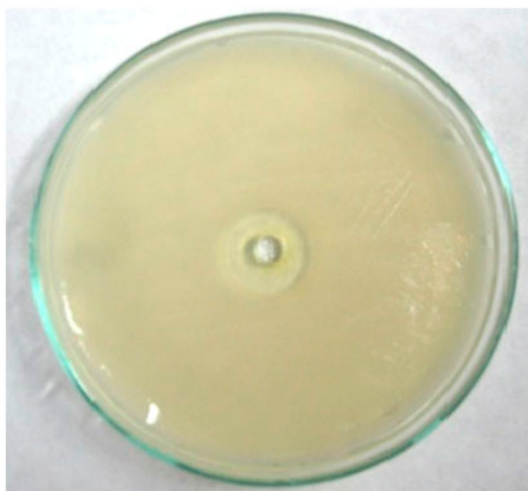
Figure 6.   Antibacterial effect of $[Co^{II}L_2(bzln)_2]$ (**1**) on *S. aureus* (MZI = 30 mm).
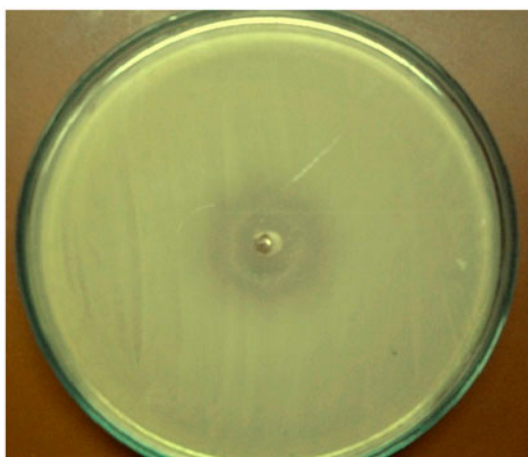

Figure 7.   Antibacterial effect of penicillin on *S. aureus* (MZI = 33 mm).

enhances the lipophilicity of the complex. This, in turn, enhances the penetration of complexes into the lipid membrane and blocking the metal bonding sites on enzymes of microorganisms, leading to increase in biological activity [43].

4. Conclusion

In two consecutive reactions, we prepared new Co(II), Ni(II), and Zn(II) complexes with the bidentate Schiff base HL = 2-((E)-(benzylimino)methyl)-4-nitrophenol. The complexes obtained, $[Co^{II}L_2(bzln)_2]$ (**1**), $[NiL_2(DMF)_2]$ (**2**), and $[ZnL_2]$ (**3**), are mononuclear with Co

and Ni in octahedral coordination by two bidentate chelating ligands L and two coligands, all in *trans* disposition, while Zn has a distorted tetrahedral coordination by two bidentate chelating L. A common feature of the three crystal structures is that they all are stabilized by π–π interactions between centrosymmetric pairs of nitrophenyl fragments generating chain-like arrangements. Antimicrobial tests showed that the synthesized compounds possess biological activity and are effective on Gram + ve but have no significant effect on Gram −ve bacterial species. However, the exact mechanism is not known and further biological studies are necessary to get a clear picture of this behavior.

Supplementary material

X-ray crystallographic data for **1**, **2,** and **3** have been deposited with the Cambridge Crystallographic Data Center as supplementary publication CCDC No. 1004450 (for **1**), No. 1004451 (for **2**), and No. 1004452 (for **3**). Copies of the data can be obtained free of charge on request at www.ccdc.cam.ac.uk/conts/retrieving.html (or from the Cambridge Crystallographic Data Center (CCDC), 12 Union Road, Cambridge CB2 1EZ, UK; Fax:+44(0)1223 336033; Email: deposit@ccdc.cam.ac.uk).

Acknowledgments

Supplemental data

Supplemental data for this article can be accessed here [http://dx.doi.org/10.1080/00958972.2014.996144].

References

[1] T.P. Yoon, E.N. Jacobsen. *Science*, **299**, 1691 (2003).
[2] G. Magadur, J.S. Lauret, G. Charron, F. Bouanis, E. Norman, V. Huc, C.S. Cojocaru, S. Gómez-Coca, E. Ruiz, T. Mallah. *J. Am. Chem. Soc.*, **134**, 7896 (2012).
[3] A. Böttcher, T. Takeuchi, K.I. Hardcastle, T.J. Meade, H.B. Gray. *Inorg. Chem.*, **36**, 2498 (1997).
[4] E. Canpolat, M. Kaya. *J. Coord. Chem.*, **57**, 1217 (2004).
[5] R.L. Lucas, M.K. Zart, J. Murkerjee, T.N. Sorrell, D.R. Powell, A.S. Borovik. *J. Am. Chem. Soc.*, **128**, 15476 (2006).
[6] P.E. Aranha, M.P. dos Santos, S. Romera, E.R. Dockal. *Polyhedron*, **26**, 1373 (2007).
[7] A.A. Soliman, W. Linert. *Monatsh. Chem.*, **138**, 175 (2007).
[8] M. Xie, G. Xu, L. Li, W. Liu, Y. Niu, S. Yan. *Eur. J. Med. Chem.*, **42**, 817 (2007).
[9] K.Y. Lau, A. Mayr, K.K. Cheung. *Inorg. Chim. Acta*, **285**, 223 (1999).
[10] R. Ramesh, M. Sivagamasundari. *Synth. React. Inorg. Met.-Org. Chem.*, **33**, 899 (2003).
[11] C.M. Che, J.S. Huang. *Coord. Chem. Rev.*, **242**, 97 (2003).
[12] P.G. Cozzi. *Chem. Soc. Rev.*, **33**, 410 (2004).
[13] K.C. Gupta, A.K. Sutar. *Coord. Chem. Rev.*, **252**, 1420 (2008).
[14] C. Goze, C. Leiggener, S-X. Liu, L. Sanguinet, E. Levillain, A. Hauser, S. Decurtins. *Chem. Phys. Chem.*, **8**, 1504 (2007).
[15] Y. Sui, D.P. Li, C.H. Li, X.H. Zhou, T. Wu, X.Z. You. *Inorg. Chem.*, **49**, 1286 (2010).

[16] A.A. Osowole, S.A. Balogun. *Eur. J. Appl. Sci.*, **4**, 6 (2012).
[17] N.S. Gwaram, H.M. Ali, H. Khaledi, M.A. Abdulla, H.A. Hadi, T.K.W. Lin, Ch.L. Ching, Ch.L. Ooi. *Molecules*, **17**, 5952 (2012).
[18] E. Gungor, S. Celen, D. Azaz, H. Kara. *Spectrochim. Acta, Part A*, **94**, 216 (2012).
[19] M. Khaled Bin Break, M. Ibrahim, M. Tahir, K.A. Crouse, A.M. Ali, T.-J. Khoo. *Bioinorg. Chem. Appl.*, **362**, 513 (2013).
[20] T.-J. Khoo, M. Khaled Bin Break, K.A. Crouse, M. Ibrahim, M. Tahir, A.M. Ali, A.R. Cowley, D.J. Watkin, M.T.H. Tarafder. *Inorg. Chim. Acta*, **413**, 68 (2014).
[21] O.B. Ibrahim, M.A. Mohamed, M.S. Refat. *Can. Chem. Trans.*, **2**, 108 (2014).
[22] S. Meghdadi, M. Amirnasr, F. Bagheri, F. Ahmadi Najafabadi, K. Mereiter, K.J. Schenk, F. Ziaee. *J. Iran. Chem. Soc.*, **11**, 985 (2014).
[23] S. Meghdadi, K. Mereiter, V. Langer, A. Amiri, R. Sadeghi Erami, A.A. Massoud, M. Amirnasr. *Inorg. Chim. Acta*, **385**, 31 (2012).
[24] S. Meghdadi, M. Amirnasr, K. Mereiter, H. Molaee, A. Amiri. *Polyhedron*, **30**, 1651 (2011).
[25] H.A. Zamani, M.S. Zabihi, M. Rohani, A. Zangane, M.R. Ganjali, F. Faridbod, S. Meghdadi. *Mater. Sci. Eng., C*, **31**, 409 (2011).
[26] B. Mondal, G.K. Lahiri, P. Naumov, S.W. Ng. *J. Mol. Struct.*, **613**, 131 (2002).
[27] (a) *Bruker Programs: SMART, SAINT, SADABS, SHELXTL*, Bruker AXS, Madison, WI (2009); (b) G.M. Sheldrick. *Program for Empirical Absorption and Other Corrections*, University of Göttingen, Göttingen (1996).
[28] G.M. Sheldrick. *Acta Cryst.*, **A64**, 112 (2008).
[29] *X-AREA, Version 1.62*, Stoe & Cie, Darmstadt (2011).
[30] *X-RED32, Version 1.31*, Stoe & Cie GmbH, Darmstadt (2005).
[31] P.T. Beurskens, G. Beurskens, R. de Gelder, S. Garcia-Granda, R.O. Gould, R. Israel, J.M.M. Smits. *The DIRDIF-99 Program System*., Crystallography Laboratory, University of Nijmegen, Nijmegen (1999).
[32] S. Magaldi, S. Mata-Essayag, C.H. de Capriles, C. Perez, M.T. Colella, C. Olaizola, Y. Ontiveros. *Int. J. Infect. Dis.*, **8**, 39 (2004).
[33] P. Mukherjee, M.G.B. Drew, A. Ghosh. *Eur. J. Inorg. Chem.*, **3372**, (2008).
[34] W.J. Geary. *Coord. Chem. Rev.*, **7**, 81 (1971).
[35] L.K. Thompson, F.L. Lee, E.J. Gabe. *Inorg. Chem.*, **27**, 39 (1988).
[36] A. Syamal, K.S. Kale. *Ind. J. Chem.*, **19A**, 225 (1980).
[37] H. Günay, A.T. Çolak, O.Z. Yeşilel, S. Keskin, O. Büyükgüngör. *Polyhedron*, **48**, 199 (2012).
[38] B.N. Sarkar, K. Bhar, S. Kundu, H.-K. Fun, B.K. Ghosh. *J. Mol. Struct.*, **936**, 104 (2009).
[39] P. Mukherjee, M.G.B. Drew, V. Tangoulis, M. Estrader, C. Diaz, A. Ghosh. *Polyhedron*, **28**, 2989 (2009).
[40] Y.F. Ji, R. Wang, S. Ding, C-.F. Du, Z-.L. Liu. *Inorg. Chem. Commun.*, **16**, 47 (2012).
[41] A.A. Nejo, G.A. Kolawole, A.O. Nejo. *J. Coord. Chem.*, **63**, 4398 (2010).
[42] N. Nishat, R. Rasool, S. Khan, S. Parveen. *J. Coord. Chem.*, **64**, 4054 (2011).
[43] Z.H. Chohan, M. Arif, Z. Shafiq, M. Yaqub, C.T. Supuran. *J. Enzyme Inhib. Med. Chem.*, **21**, 95 (2006).